This paper is a pre-print of 10.1109/TTE.2019.2914890 accepted by IEEE trans. on Transportation Electrification on 8th of May 2019 and as such is subject to IEEE copyright.

A novel methodology for macro-scale, thermal characterisation of carbon fibre reinforced polymer for integrated aircraft electrical power systems

Catherine E. Jones, Andrew W. Hamilton, Patrick J. Norman, Alison Cleary, Stuart J. Galloway, Robert Atkinson, Graeme M. Burt, *Member IEEE*, Craig Michie, *Member IEEE*, Ivan Andonovic, *Senior Member IEEE*, Christos Tachtatzis, *Senior Member IEEE*.

***Abstract*— Carbon fibre reinforced polymer (CFRP) is increasingly used for aero-structure applications due to their high strength-to-weight ratio. The integration of the on-board electrical power system (EPS) with CFRP is challenging due to the requirement to thermally and electrically isolate these systems to meet existing safety standards. By capturing the thermal characteristics of CFRP at a macro (component) scale for CFRP components, it is possible to understand, and design for, the increased integration of the EPS into CFRP aero-components. A significant challenge is to develop a macroscale characterisation of CFRP which is not only of an appropriate fidelity for compatibility with systems level models of an EPS, but can be used to represent different geometries of CFRP components. This paper presents a novel methodology for capturing a transient, macro-scale thermal characterisation of CFRP with regards to component lay-up and geometry (thickness). The methodology uses experimentally derived thermal responses of specific resin and ply orientation CFRP samples to create generalised relationship for the prediction of thermal transfer in other sample thicknesses of same material type. This methodology can be used to characterise thermal gradients across CFRP components in aircraft EPS integration applications, ultimately informing the optimised integration of the EPS with CFRP.**

***Index Terms*— Carbon fibre reinforced polymer, electrical protection, thermal characterisation, aircraft electrical power systems, aerospace.**

I. Introduction

There is a continuing upwards trend for the use of composite materials, in particular, carbon fibre reinforced polymers (CFRP) for aircraft structures due to their superior mechanical properties compared to traditional metal structures. This results in lower airframe weights and hence fuel burn. However, the increased use of CFRP strongly influences the wider holistic aircraft design, including the electrical power system (EPS) [1]. In particular the poorer electrical and thermal properties of CFRP compared to metallic structures [2, 3], has had a significant influence on how the EPS is integrated with composite aero-structures.

The selection of cable size for an aircraft EPS is governed by the rated maximum temperature for a conductor which is influenced by the environment that a cable is operating in [4]. To prevent thermal damage to surrounding materials under abnormal (fault) conditions, cables require thermal insulation and appropriate physical separation [5]. In the case of integrated EPS with aircraft structures, surrounding materials would include CFRP structures. In addition the relatively poor electrical conductivity of CFRP results in significant Joule heating during electrical current conduction [2], as well as poor shielding against electromagnetic interference (EMI) and poor electromagnetic compatibility (EMC) [6]. At present this requires the addition of metallic structures to provide electrical current return [7, 8], metallic meshes for lightning strike protection and EMC shielding [9], and extensive use of heavy cable harnesses to route cables around CFRP structures [10].

To date, the integration of the EPS with composite structures has focused on these electrical response of CFRP [2, 11, 12, 13], in particular to the degradation of CFRP due to localised increase of temperature to above the glass transition temperature of the resin due to Joule heating during electrical conduction [2, 14]. However, heating CFRP to temperatures below the glass transition temperature is also known to have an influence on the mechanical performance of the CFRP [14].

Whilst existing methods to integrate the on-board EPS with the CFRP structure of an aircraft are safe, they require additional metallic structures. There is an opportunity to reduce the EPS system mass if the thermal response of CFRP on a macro (component scale, from mm up to 10s of m [15] due to sustained Joule heating is better understood. Firstly, in the case where a fault is detected and removed before glass transition temperature is reached. Secondly, to enable the possibility of

C. E. Jones, P. J. Norman, S. J. Galloway and G. M. Burt are with the Advanced Electrical Systems (AES) group of the Dept. of Electronic and Electrical Engineering (EEE) of the University of Strathclyde, Glasgow, United Kingdom, G1 1RD.

(e-mails: catherine.e.jones@strath.ac.uk; patrick.norman@strath.ac.uk; stuart.galloway@strath.ac.uk; graeme.burt@strath.ac.uk)

A. W Hamilton, A. Cleary, R. C. Atkinson, C. Michie, I. Andonovic and C. Tachtatzis are with the Centre for Intelligent Dynamic Communications (CIDCOM) of the Dept. of EEE of the University of Strathclyde, Glasgow, United Kingdom, G1 1RD

(e-mails: andrew.w.hamilton@strath.ac.uk; alison.cleary@strath.ac.uk; robert.atkinson@strath.ac.uk; c.michie@strath.ac.uk; i.andonovic@strath.ac.uk; christos.tachtatzis@strath.ac.uk).

intentional conduction of electrical current through CFRP. Thirdly, such understanding is needed to inform the layout and sizing of electrical cables over CFRP to enable appropriate thermal management system design [16], including where cables must pass through confined spaces in composite structures [17], [18]. In all of these cases, the optimisation of the thermal system design will provide an opportunity for mass reduction. The integration of the thermal characteristics of CFRP with existing electrical models of CFRP [2] and the EPS will enable studies to inform and optimise system design, both in terms of EPS architectures, but also choice of lay-up and shape of CFRP structures.

Critical to this is that the level of complexity of the thermal characterisation of the CFRP is such that it maps the appropriate complexity level of the modelling paradigm for modelling aircraft EPS, as set out in SAE AIR 6326 [19], thus enabling systems level transient studies to take place. Thermal models of carbon fibre composites are typically based on numerical modelling methods [20]–[23], which are too complex (require too small a simulation time-step) for transient, systems studies according to [19]. Numerical models can be used to identify thermal response of a CFRP component, the response is for a particular component geometry. Therefore, there is an opportunity to develop a method to thermally characterise CFRP to enable the thermal response of CFRP to sustained heating to be captured at an appropriate complexity, to then be able to estimate the thermal response of different geometries, thus informing the integrated design process.

CFRP is a complex, heterogeneous material comprising of carbon fiber and a resin matrix. The thermal response of CFRP is sensitive to lay-up, choice of carbon fibre and resin, volume fraction of fibre, imperfections in the internal structure, surrounding temperature and geometry of the structure [24]–[29]. The layup and shape of CFRP, alongside local environmental conditions, vary in different parts of an aircraft. Hence it is not a bespoke model of a particular CFRP lay-up which is required, rather a methodology to enable the capture of the thermal characteristics of a CFRP layup, from which an appropriate representation of the thermal response of CFRP that can be integrated into EPS models can be derived. The aspect of variation of thermal response with component geometry is particularly applicable to aerospace where thickness of a component may offer another opportunity to optimise the size of a component.

This paper provides an experimental methodology to derive a component-scale thermal characterisation and datasets for a CFRP layup, where the derived characterisation can be extrapolated for different thicknesses and sizes of CFRP structures, at a level of complexity suitable for integration with aircraft EPS design. The method is demonstrated by using the proposed methodology to thermally characterise aerospace grade 8552/IM7 UD [0º] CFRP [30]. By focusing on a basic, aerospace grade CFRP, the resulting thermal characterisation provides a strong platform for future extension to more complex lay-ups and resin matrices which contain additives (e.g. carbon nanotubes) [31] as well as the impact of variation in the shape and thicknesses of CFRP structures.

The remainder of this paper is organised as follows: Section II of this paper discusses the relevant properties of CFRP, their potential impact and reviews the theoretical thermal modelling approaches presented in the literature; Section III describes existing methods of thermal characterisation; Section IV presents a testing methodology that is appropriate for quantifying thermal properties and a characterisation system that can be used to predict behaviour in varying structural conditions that can be used in the design and implementation of the application described. Finally, Section V presents discussions and Section VI conclusions and future work.

II. Thermal Properties of CFRP

A. Complexity of CFRP

CFRP is a heterogeneous material comprising a resin (usually a thermosetting epoxy) forming the matrix and carbon fibre (CF) providing tensile strength. Aerospace grade pre-preg CFRP has a volume fraction for carbon fibre of circa 55 % - 60%, the type of carbon fibre chosen has a high modulus and strength [32] and the layup can either be woven or unidirectional (UD). This paper will focus on UD [0°] CFRP, where fibres of CFRP lie parallel within each ply, held in place by the resin

Thermally, CFRP is a complex material due to thermal resistance and localised heating at the interface between the carbon fibre and the resin matrix [21], [33]. In addition the thermal conductivity of carbon fibre is much higher than resin, leading to a strong interdependency between lay-up and thermal properties [23], [29]. The localised fibre fraction volume content can be highly varied across a given sample on the micro-scale (10s of µm [15]) due to variation in the curing process, resulting in imperfections through the CFRP [34]. In addition, misalignment (waviness) of aerospace grade carbon fibre results in non-uniform distribution of contact points between fibres, both cross-ply and along ply, as well as gaps between fibres at the micro-scale which are resin rich [35], [36]. The different thermal properties of the carbon fibre and resin, combined with different lay-ups and imperfections in the CFRP result in the CFRP having highly complex, micro-scale thermal properties, which are then difficult to extrapolate to the macro-scale. A significant challenge for integration of CFRP structures with the aircraft EPS, is to capture the overall thermal characteristics at a component-scale, at a level of complexity compatible with a systems level computer simulation tool.

B. Thermal and Electrical Response of CFRP

The relatively high electrical and thermal conductivity of carbon fibre compared to resin results in UD CFRP having highly anisotropic thermal and electrical properties [2], [11], [12], [37]. If electrical current is injected into CFRP (for example, due to an electrical short circuit to ground), localised Joule heating occurs along sections where the fibre strands are conducting electrical current [2], [11], [38]. Existing aerospace industry standards do not allow the intentional conduction of electrical current through CFRP on aircraft [39], due to the relatively high electrical resistance of CFRP compared to metals. The electrical power, P_d *(W)*, which is dissipated as heat in a section of CFRP with an electrical resistance, R_{CFRP} *(Ω)*, conducting an electrical current, *I (A)*, can be defined as

$$P_d = I^2 \cdot R_{CFRP} \quad . \tag{1}$$

CFRP may also be heated due to close proximity to a cable. The sizing of electrical cables is influenced by the allowable heat dissipation in cables, combined with EPS impedance [16]. To meet airworthiness standards, there must be adequate physical separation between cables to ensure that hazardous conditions in the event of a fault conditions do not arise and to ensure that there is adequate cooling between cable bundles [5], [18]. If the thermal response of a CFRP structure is known, then the optimum layout of the EPS can be developed and requirements for necessary thermal management systems and insulation derived.

In the case of a localised temperature increase in CFRP due to conduction of electrical current or proximity to a heat source (e.g. cable) the difference in temperature, ΔT *(°C)*, between the CFRP, T_{CFRP} *(°C)*, and the local ambient temperature, T_a *(°C)*, can be expressed as,

$$\Delta T = (T_{CFRP} - T_a) = \frac{P_d \cdot d}{\lambda \cdot A} \tag{2}$$

where P_d *(W)* is the electrical power dissipated in the section of CFRP, λ *(W/m°C)* is the thermal conductivity, and A *(m²)* is the cross-sectional area, and d *(m)* the distance that the current is passing through.

Whilst (1) and (2) can be used to estimate the localised temperature increase through a section of CFRP, there is no indication of how quickly the temperature will rise, or the speed at which the dissipation of heat through the component level region will occur. Further, it is known from the literature that thermal conductivity and heat capacity varies with temperature and although this relationship can be assumed to be linear [25], this temperature dependence significantly increases the complexity of the development of a thermal model for CFRP. An estimation of the relationship between CFRP geometry and temperature response is required. However due to the variation in thermal properties for different layups and resins for CFRP, it is more useful to develop a methodology to capture thermal characteristics, rather than a characterisation that is bespoke to a specific CFRP layup and resin.

C. Review of existing thermal models for CFRP

Thermal models for CFRP in the literature fall into two broad categories: those based on component-scale heterogeneous analytical models, and those based on homogenisation of the CFRP using numerical modelling methods. The analytical methods based on the work of Maxwell and Raleigh are only valid for CFRP lay-ups with a low volume fraction of CF, as these do not take interfacial thermal interactions between the fibres and resin matrix into account [33], [40]. The Hasselman and Johnston model [33] has adapted the Raleigh model to take interfacial thermal interactions into account, but has only been verified for low volume fractions of carbon fibre. Hence these are not suitable for aerospace grade CFRP which has a high volume fraction of CF.

An alternative approach is to model the system as a parallel thermal resistor network, using the law of mixtures to estimate thermal conductivity [41], [42]. This gives good results for directions parallel and perpendicular to fibres, but cannot be used to confidently predict thermal characteristics if the heat source is not parallel or perpendicular to the fibres [26], [42]. This is because the rule of mixtures models the CFRP as a 2 dimensional, rather than a 3 dimensional system which neglects thermal interactions in the transverse (through thickness) direction [42].

Results from homogenised macro-scale models based on numerical modelling methods such as finite element modelling, have been demonstrated in the literature to give a good representation of the thermal behaviour of UD CFRP materials with high fibre content [20], [23], [37], [43], [44]. The methods presented develop a thermal micro-mechanical model of a unit of the CFRP at a micro scale, and then directly use this to model the CFRP as a homogenous material at a macro-scale e.g. [23], or create an intermediary meso-scale model (a few mm [15]) which is then used to develop a macro-scale model e.g. [37].

The implementation of numerical modelling is challenging. Firstly, the selection of the size of the unit section of heterogeneous CFRP for the unit model must be carefully selected to ensure it will give a good average indication of the properties of the CFRP when extrapolated to a macro-scale model [43], [45]. If the unit section size wrongly selected, then non-periodic variations in the system (e.g. variations in resin thickness due to variable gaps between CFs) will result in errors of up to 15% in the final model [29]. Secondly, numerical modelling methods require significant computational effort: thermal interactions between CF and resin, and between the individual unit blocks which form the macro-model must be considered at a three-dimensional (rather than 2 dimensional) level [21], [22], [42], [44]. Ultimately each model is only valid for the specific lay-up that it represents. Numerical models for inductive heating of CFRP are also well developed, however these have been developed for high frequency (400 kHz) inductive heating applications [46]. This is a much higher frequency than would be expected for a more-electric aircraft power system, where AC system frequency typically ranges from 320-800 Hz [47], [48] and the switching frequency of power electronic converters can be up to 20 kHz [49].

The results presented in the literature, for UD CFRP, have utilised the numerical modelling method to develop macro-scale models, from which the transient thermal response e.g. [20], [23], [37] for a predetermined size of CFRP panel can be estimated. Hence, in order to compare the thermal response of different sizes of structures, the numerical model must be re-run.

Critically for the design of integrated systems, the level of complexity of numerical based models, and the resulting high fidelity required for such computational models, is not compatible with the level of modelling complexity and computational time step required for systems level modelling for an EPS. As is set out in SAE AIR 6326 [19] there are four levels of modelling for an aircraft EPS: Architectural, Functional, Behavioural and Device Physical. The two levels of modelling of interest for transient EPS studies, are Functional, which uses average models of systems (e.g. no switching models of power electronic converters) at system and sub-system level, and Behavioural, which uses fully (idealised)

switching models to carry out sub-system analysis, including detailed power quality and harmonics analysis. The numerical thermal models of CFRP described in the literature will fit within the Device Physical level of modelling, which includes

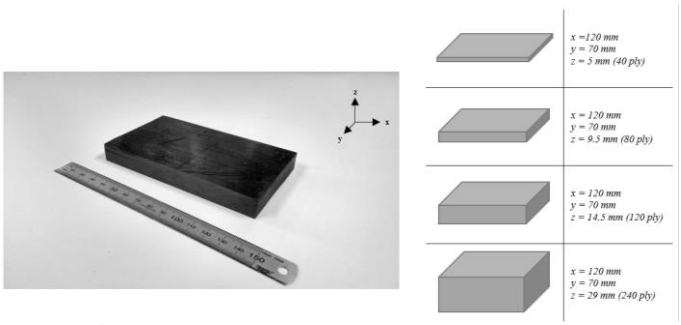

Fig. 1. Left – UD [0°] CFRP sample 120 ply thick used in validation experiments. *Right* – dimensions of all samples used, with materials consisting of UD [0°] Hexcel 8552 IM7 with a 1.77 g/cm^3 fibre density and nominal fibre volume of 57.7%.

multi-physics modelling and detailed component design, however it will not enable systems or sub-systems level modelling (Behavioural and Functional levels) which will enable full system design and physical layout. Hence there is a need for an approach that will map to the systems level of modelling which allows for comparison of different geometries of CFRP structures. Experimental methods are presented in the literature for capturing the thermal conductivity of a material at a macro-level e.g. [50] and capturing the transient thermal response e.g. [23]. However, these do not convert the captured results into a transient characterisation that can be used to estimate the thermal response of other structures of a similar lay-up but different geometry, which can be used in systems level modelling to estimate the thermal response of CFRP to EPS induced heating.

III. Review of Thermal Characterisation Methodologies of CFRP

Experimental methodologies of thermal characterisation presented in the literature focus predominantly on estimating the thermal conductivity (or thermal resistance), with a fixed, constant temperature. For example, the modular differential scanning calorimetric methodology requires reference samples with a known thermal conductivity. This is also limited in the range of temperatures over which it is valid, and measures the thermal properties of a small sample size (10 – 100 mg), hence any imperfections will not be taken into account [51]. Laser flash analysis (LFA) measures the response of a composite to a pulse of energy, to capture thermal diffusivity, from which thermal conductivity can be calculated [52], [53]. However, achieving the correct conditions in the laboratory to obtain accurate results from the laser flash methodology is known to be difficult [52]. It also requires measurements to be made at a small scale (a few mm), rather than a macro-scale [53] which may result in errors due to the heterogeneous nature of the material during extrapolation to macro scale. Furthermore, LFA requires knowledge of the specific heat and density of the material [52], which if not accurately known, significantly reduces confidence in the final estimation of the thermal conductivity to as low as 10% [45]. Finally, LFA only provides the thermal diffusivity for a specific temperature, and hence measurements must be made at a range of temperatures to extract the relationship between temperature and thermal conductivity for the CFRP lay-up under investigation [25].

Alternative standard methodologies for investigating thermal properties to understand the thermal response of CFRP to Joule heating due to electrical current conduction and hence inform EPS integration, are described in standards D5470-17 [54] which measures the thermal impedance, C518-17 [55] to measure steady state thermal transmission, and C177 -13 [56] to measure the steady state heat flux. However, these methodologies are focussed on the captured thermal properties of a composite material by placing it between a heat source and a heat sink. Whilst these methodologies do allow for the variation in geometry and thickness to be taken into account, for example by consideration of (1) and (2), these equations cannot simply be utilised without an understanding of how the thermal properties vary with temperature. The basic experimental methodology employed of placing a material to be tested between a thermal source and a heat sink, provides a starting point for a methodology to capture data to develop a characterisation of heat transfer through CFRP as the geometry of the CFRP is varied.

IV. Novel Thermal Characterisation Methodology

An experimental methodology is presented to develop a thermal characterisation of CFRP which models the dissipation of heat through different geometries of CFRP. The selected methodology is based on introducing thermal energy along different axes (due to anisotropic material properties) from a thermal source. This is where thermal energy is introduced via a surface or from a single point/conductive line source that propagates through the component. By introducing thermal energy along different axes, it was also possible to investigate the effect of fibre direction on the thermal response of CFRP representative of the conditions in electrical protection settings. The methodology of the characterisation process is summarised in Fig. 2. The methodology uses 3 samples of differing thicknesses that can be experimentally characterised through thermal testing.

The thicknesses of samples are selected to match the expected component thicknesses that would be created with this CFRP material. The samples are then tested for thermal response along each sample axis multiple times to ensure repeatability. The measured responses (time constant and final temperature) are then used to derive a thermal response as a function of thickness. In the context of the work described, the time constant was defined to be the time taken to reach 63.2% of the final set point as used in signal analysis and control applications. This allows the prediction of the thermal response of other samples thickness of the same CFRP material within the range of thickest and thinnest test samples.

To validate the thermal characterisation, untested samples are then characterised so that the actual thermal response can be used to evaluate the predicted response and hence the accuracy of the derived thermal characterisation and appropriateness of the methodology. The number of untested samples that are

characterised is dependent on the required confidence level of the final thermal characterisation.

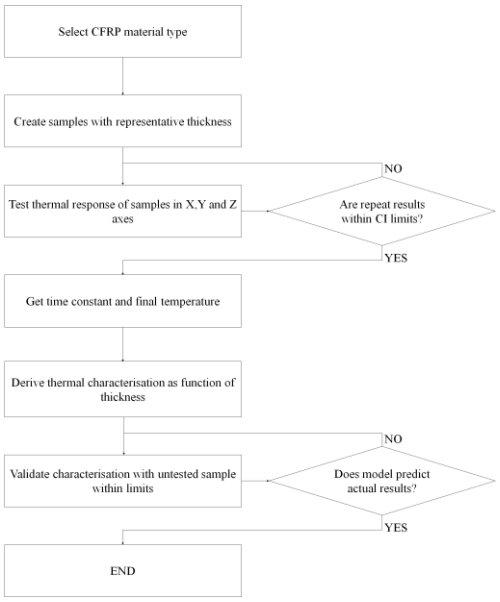

Fig. 2. Methodology of macro-scale characterisation of CFRP material based on thickness with capture of experimentally derived thermal time constants and asymptotic final temperature per axis, including decisions regarding confidence interval (CI) limits, and validation of the resulting thermal characterisation.

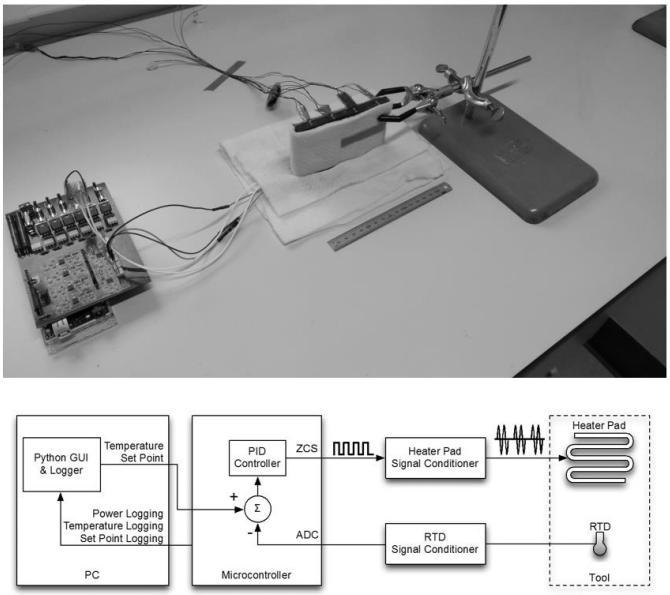

Fig. 3. *Top* - Experimental setup with controller (*left*), carbon fibre panel with insulation applied and 4 RTD's on opposing thermal surface (*centre*). Y axis direction is under test. *Bottom* - Control system for temperature feedback and heater power modulation using a microcontroller and PC for setpoint definition/data logging.

A. Samples

Fully cured UD [0°] Hexcel 8552 IM7 CFRP aerospace grade composite was used in the experimental case study presented in this paper. This material used an amine cured toughened resin with unidirectional, PAN-based fibres with a 1.77 g/cm^3 fibre density and nominal fibre volume of 57.7%, which was consistent across all 4 samples. A set of 4 samples were created with a ply number of 40, 80, 120 and 240, with all layers orientated in the same direction and shown in Fig. 1. The samples were cut to 120 x 70 mm in the 'X' and 'Y' directions, with the 'Z' direction determined by the ply number (40 plies is approximately equivalent to 5 mm).

B. Experimental Equipment

A silicone rubber heater mat was used to introduce thermal energy into the samples. The heater pad was driven by a modulated 240 VAC input that was controlled using a Proportional-Integral-Derivative (PID) controller (tuned using Ziegler-Nichols) on a local microcontroller (MC) that could receive signals from a computer so that customised thermal profiles could be applied [57]. Prior to conducting the tests, the heater pad was monitored with a thermal camera to determine the spatial variation of heat dissipation. It was found that the heater pad had a 2σ of 0.5°C at 20°C and a ±2σ of 1.2°C at 150°C. For the set point of 20°C this meant that 95% of the heater pad surface area was within ±0.5°C after 2 s of receiving the given set point.

The MC was an 8-bit Atmel ATMega 328 with 6 Analogue-to-Digital Converters (ADC) and 1 digital output to control the scheduling of the heater pad. The ADCs were single-ended successive approximations and their channels were multiplexed, providing a 10-bit resolution.

The system used class A, pt100 resistive temperature detectors (RTD) with a signal conditioner to provide temperature feedback within ± 0.25°C. This type of temperature sensor provided a linear resistance-temperature relationship within the experimental temperature range (0-180°C) profile [58]. The sensor would report a resistance value of 100Ω at 0°C if provided with a 2.5V and 1mA supply voltage and current. The conductive heater mat used was rated at 1.2W/cm^2 using a 240VAC supply. The MC sampled at a frequency of 5Hz and returned the rolling windows average of these values (equating to a 1 Hz sampling on the PC side) to reduce ADC noise [59]. The architecture of the heating system is illustrated in Fig. 3.

C. Laboratory Environment

The experiments were conducted in a temperature and humidity controlled laboratory in which the ambient temperature was between 20-21°C and the humidity was within the range of 36-40% (relative humidity for 20 – 21°C).

D. Temperature Profile

A single thermal step change was used to characterise the samples where the heater pad temperature would initially stabilise at 30 °C for 30 s before increasing the setpoint to 150°C. The setpoint was selected to prevent damage within the samples to ensure repeatable measurements as CFRP can become damaged at temperatures above 180°C, as above this temperature localised heating above the glass transition temperature (200 °C) of the material may occur. A single step was selected as this is representative of the case where an electrical fault develops within the composite resulting in a rapid temperature rise. From this response, the time constant for each system was estimated (time taken to reach 63.2% of the final temperature), and of the thermal delta between each opposing surface could be measured [60]. The coefficient of thermal expansion (CTE) for Hexply 8552 [0°] was taken to be

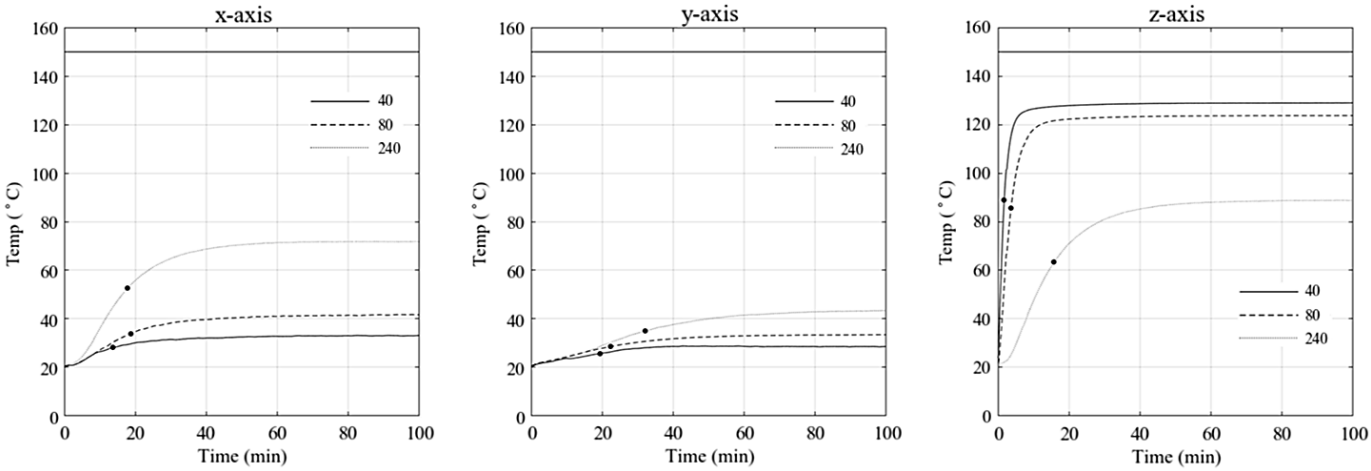

x-axis 40 ply σ = 1.2℃	*y-axis 40 ply σ = 1.1℃*	*z-axis 40 ply σ = 1.0℃*
x-axis 80 ply σ = 1.2℃	*y-axis 80 ply σ =1.3℃*	*z-axis 80 ply σ = 0.9℃*
x-axis 240 ply σ = 1.1℃	*y-axis 240 ply σ = 1.2℃*	*z-axis 240 ply σ = 1.1℃*

Fig. 4. Summary of thermal responses for each experiment grouped by axis (each trace is the average of 5 individual tests). Solid lines represent 40 ply samples, dashed lines represent 80 ply samples and dotted lines represent 240 ply samples. The setpoint (SP) of 150℃ that is shown in black at the top of each plot. The time constant (τ) for each trace is indicated by a dot. In the tabulated columns below the plots are the standard deviations for the 5 sets for each experiments are shown. For example, the x-axis 40 ply sample experiments were repeated 5 times and the standard deviation of the temperature readings was found to be 1.2℃

16.73 µm/m°C from [61], however as the derived change in volume from ambient to 150°C would result in an increase of volume by 0.217%, the effect of CTE was assumed to be negligible for smaller size components.

E. Experimental Procedure

A sample was wrapped securely with fleece insulation on the non-test faces. The sample was placed with one exposed face directly on the heater pad and secured with a clamp (see Fig.3). The opposing face to the heated surface was instrumented with 4 RTDs, attached using thermal tape, to measure the thermal response when heating. The 4 RTDs were secured to the opposing face at evenly spaced intervals along the central axis (for example, when testing thermal conduction along the 'Y' axis the 4 RTDs were placed at 17.5 mm intervals in the centreline of the 'X' axis, as illustrated in the top of Fig.3). This face was not insulated with fleece (as can be seen in Fig.3) and hence provided a representative heat sink where thermal energy could be partially dissipated whilst measuring the response.

An additional RTD was used to provide atmospheric temperature feedback throughout the experiment to verify that it remained between 20 – 21℃. The thermal step input signal was communicated to the MC (from a PC in the laboratory), with the MC controlling the temperature of the heater pad. The 150℃ set point was maintained for 120 min, at which point the power to the heater pad was switched off and the sample was allowed to cool to ambient temperature. The procedure was repeated 5 times for each sample, for each X, Y and Z orientation and so 15 tests were carried out per sample. In all experiments, a single step input of 150℃ was used and the starting temperature was within the range of 20 – 21℃ (both heater pad and ambient temperature). Each set of 5 experimental repetitions for the X, Y and Z orientations per sample were evaluated for repeatability by evaluating the standard deviation (σ) across each set.

V. Results

The controller returned thermal measurements (℃) from each RTD at a frequency of 1 Hz. The thermal readings across all 6 RTDs were associated with a common timestamp. The parameters for the samples for 40, 80 and 240 ply are shown in Table I.

A. Initial Processing and Data Representation

Each of the 60 datasets were plotted (RTD measured temperature and step input against time). The 5 repetitions for each experiment were analysed to determine the repeatability of the experiments by assessing the spread of values over the time period (see Fig. 4). The time constant was derived by assessing the time taken for the thermal step response to reach 63.2% of the final (asymptotic) temperature. In Fig. 4, the summary of the thermal profiles obtained from each experiment is shown. Each individual trace represents the average of 5 separate experiments. Solid, dashed and dotted lines represent 40, 80 and 240 ply experiments, respectively.

The time constant (τ) for each trace is indicated by a dot and the set point used to drive the heater pad and thermal transfer onto the sample is shown at the top with a flat line. The results presented in Fig. 4 indicate the non-linear relationship between the thickness of a sample with both the time taken for heat to propagate through the sample and the final temperature reached. This further indicates the mathematical complexity associated with modelling this response, and justifies the need for an experimental approach to characterising the material. The thermal characterisation presented in this paper fits with the presented models of macro-scale research where the asymptotic final temperature follows an approximate exponential function when responding to a thermal step input [24].

This paper is a pre-print of 10.1109/TTE.2019.2914890 accepted by IEEE trans. on Transportation Electrification on 8th of May 2019 and as such is subject to IEEE copyright.

1) X Direction

The X direction corresponded to the along ply orientation and was also the largest distance the thermal step response was measured across (120 mm). Theoretical thermal conductivity is highest along fibres rather than across due to the presence of resin and non-uniform contact between threads. It can be seen that the smallest thermal delta between the heater pad and the monitored opposing face was observed in the 240 ply sample experiments. This was expected as the proportion of the heated area (the section of sample where the heater pad was in contact) was larger as a percentage of the non-heated surface area (7.9%), as shown in Table I. This meant that a larger surface area was available to introduce conductive thermal energy. The 40 ply sample had a heat/loss percentage of 1.9% which would reduce the total thermal energy induced at the point of measurement on the opposite face. The difference in time for each sample reaching the asymptotic final temperature followed a similar pattern when considering each time constant.

TABLE I
SUMMARY OF HEATED SURFACE AREA AND FINAL TEMPERATURE FOR EACH SAMPLE AND DIRECTION

	Ply #	40	80	240
X	Heated Area (mm²)	350	665	2030
	Loss Area (mm²)	18350	19745	25790
	Heat/Loss %	1.9	3.4	7.9
	Final Temp (°C)	32.9	41.5	72.3
	Time Constant (s)	828	1140	1067
	2σ (°C)	0.81	0.79	0.89
Y	Heated Area (mm²)	600	1140	3480
	Loss Area (mm²)	18100	19270	24340
	Heat/Loss %	3.3	5.9	14.3
	Final Temp (°C)	28.3	33.2	44.3
	Time Constant (s)	964	1220	1929
	2σ (°C)	0.80	0.85	0.92
Z	Heated Area (mm²)	8400	8400	8400
	Loss Area (mm²)	10300	12010	19420
	Heat/Loss %	81.6	69.9	43.3
	Final Temp (°C)	128.9	123.7	89.1
	Time Constant (s)	216	317	943
	2σ (°C)	0.99	1.10	1.31

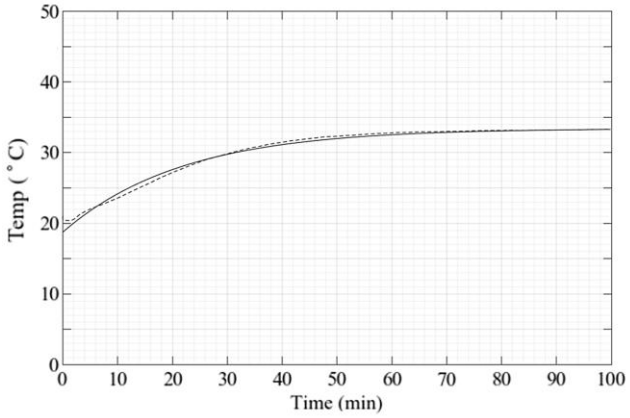

Fig. 5. Approximation of step response for an 80 ply sample along the Y axis.

2) Y Direction

The Y axis experiments measured thermal transfer over 70 mm but in the cross ply direction. Theoretically the thermal transfer would be lowest (compared with X and Z axes) due to the lower thermal conductivity between carbon strands and resin, in contrast to the X axis. It can be observed in Fig. 5 that the Y axis followed a similar pattern to the X axis, where the smallest thermal delta was observed in the 240 ply samples due to the heat loss percentages. The asymptotic final temperatures were all significantly lower than the corresponding X axis experiments due to the far lower thermal conductivity in this direction.

3) Z Direction

The Z axis offered an interesting combination of experimental parameters as the thermal delta was measured over a far shorter distance of 5-29 mm (depending on sample) and the heated area was constant for each sample thickness. This was also the through-ply direction (heat was transferred from one ply layer to the next). Due to the composition of UD [0°] there is no difference in the material thermal properties with the cross ply (Y axis) direction as there is no weave/weft to alter the strand/resin configuration. When observing the results, it was found that the 40 ply samples had the smallest thermal delta in contrast to the X and Y axes. This was due to the short overall distance and the highest heat/loss percentage (see Table I), despite the lower theoretical material thermal conductivity of the cross thread direction.

B. Ply-Thermal Relationship

The data obtained from the experiments was used in the derivation of a ply-thermal characterisation for prediction of thermal transfer in other CFRP structure geometries. The relationship between thermal conduction and sample thickness is critical to electrical protection and layout of the EPS: by accommodating for thermal transfer, electrical protection systems have deeper insight into the thermal capacity of a given structure influencing the development of appropriate electrical fault detection and protection systems, and optimising the layout of an EPS on a composite structure.

1) Approximation of Step Response

The first stage was to approximate the step response of each case using an appropriate function. All of the experiments had a similar response where the surface temperature would change slowly in the initial stages, followed by a period of rapid temperature increase that would then reduce as the final asymptotic point was reached. An exponential function was found to be the most appropriate approximation for each experiment (adjusted r^2 = 0.99 or higher),

$$f(t) = a \cdot e^{bt} + c \cdot e^{dt} \quad (4)$$

where $f(t)$ is temperature (°C), t is time (s) and (a, b, c, d) are coefficients that modify the shape of the function such as the asymptotic final value or the rise time. Each experimental dataset used (4) as a base function for curve fitting within the MATLAB Linear and Non-linear Regression Toolbox [62] and the values for each coefficient (with a 95% confidence interval) was found. An example of approximating the step response for a 40 ply sample in the Y axis is shown in Fig. 5. As the coefficients (a, b, c, d) define the shape of the step response for each experiment, it is possible to use these values to derive a generalised relationship. The assumptions for this generalised

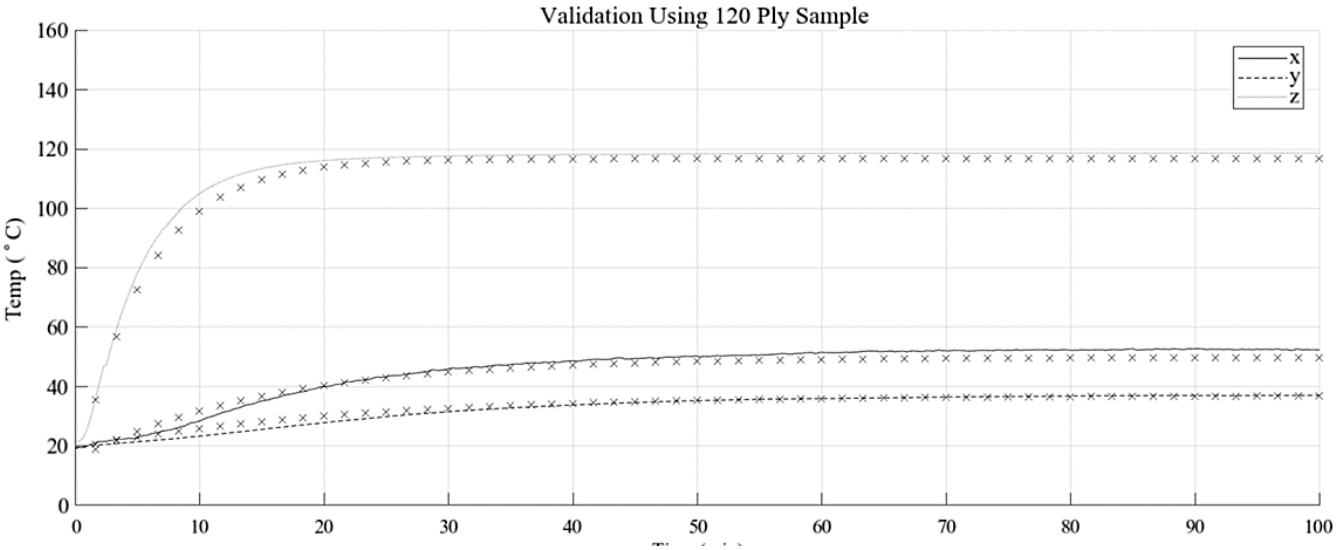

Fig. 6. Example of the thermal response for the predicted 120 ply sample response using the ply-thermal characterisation (shown by 'x' marks), compared with the actual experimental results for each axis.

relationship would be based on a component between the ply thickness (40 and 240 ply) with same layup, resin system, atmospheric conditions and conductive surface heat transfer. The complexity of the material is such that (4) is a compromise between modelling the response with one single equation, with a small amount of error, and modelling the response with two equations, one for the initial rise, and one for the steady state. It was decided that the error of 5 % was sufficiently small to justify modelling the system with a single equation.

2) Derivation of Step Response Coefficient Relationship and Ply Number

As individual sets of exponential coefficients (*a, b, c, d*) were found for each experimental setup, a general relationship based on ply number (sample thickness) and these coefficients could be derived for each axis. A two-term power series model was selected to fit each coefficient value,

$$g(n) = p1 \cdot n^2 + p2 \qquad (5)$$

where *g(n)* is coefficient value *a*, *b*, *c* or *d* from (4), *n* is the ply number and (*p1, p2*) are coefficients.

The values of coefficients *p1* and *p2* were derived, using (5), for all the experimental coefficients from (4). This allowed a relationship to be established between sample thickness and the each of the corresponding coefficients, *a*, *b*, *c* and *d* (see Fig. 7). With *p1* and *p2* known, thermal step response of the part of a given sample thickness can be predicted.

3) Application of Ply-Thermal Relationship and Validation

The characterisation derived using (4) and (5), allows the estimation of the thermal step response for any number of ply in the layup within the range of 40 and 240 ply. To validate the estimated thermal response of the characterisation, additional experiments were conducted for a test sample of 120 ply using the same methodology as described in Section IV and it was repeated 5 times. The predicted thermal response obtained from the characterisation was subsequently compared to the experimental response as it can be observed in Fig. 6.

The metrics of the characterisation (final temperature and time constant) were found for predicted/actual results and are summarised in Table II (the 95% confidence intervals between repetitions are stated in brackets using the t-distribution used for 5 or less samples).

VI. Discussion

The derived characterisation served as an example of the type of thermal prediction possible, based on full sized samples where thermal transfer is a function of sample thickness direction.

A. Validation of characterisation

By comparing the derived characterisation to data obtained from a differing sample thickness, the performance of the derived characterisation was assessed. Overall the characterisation approximated the response of the 120 ply samples with the largest final temperature error for ± 4.4℃ for the Z axis and time constant error of ± 3 min for the Y axis. When considering the CFRP characteristics as detailed in Section II, the Y and Z directions were most likely to produce errors in prediction due to the non-uniform contact of electrical and thermally conductive carbon fibre strands.

The same effect is found in the Z axis, but due to the larger total thermal energy transfer from the larger conductive surface area, the effect is reduced when compared to the Y axis. In the X axis, the energy is largely conducted along the fibres continuously and so the presence of resin regions has smaller impact and allows for more efficient thermal transfer. These results show that the derived characterisation is able to predict with reasonable accuracy the expected final temperature and time constant which would provide the main characteristics required to assess the thermal response.

For electrical protection systems in aerospace, the sample thicknesses represented the extremes that would be found in structural CFRP. Consequently, the validity of the derived characterisation in the range 40 and 240 plies is adequate.

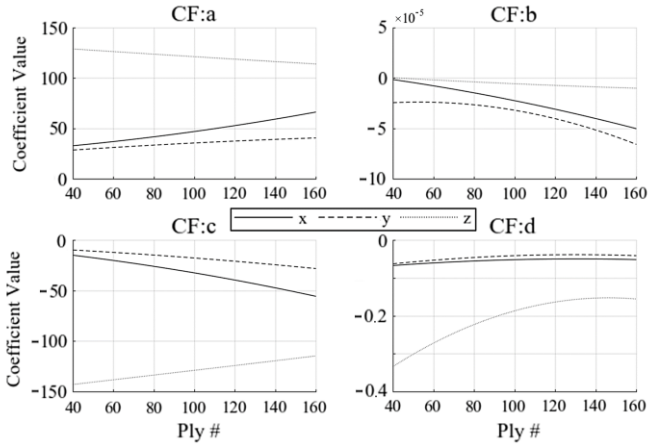

Fig. 7. Derivation of a generalised relationship between exponential function coefficients and ply number. Each lines, solid, dashed and dotted, represents the coefficient curve for the X, Y and Z axes respectively. The coefficient (CF) in question is labelled above each plot.

TABLE II

COMPARISON OF PREDICTED AND ACTUAL FINAL TEMPERATURE/TIME CONSTANT FOR 120 PLY SAMPLES

Axis	Metric	Predicted	Actual
X	Final Temperature (°C)	49.9 (±3.4)	52.2
	Time Constant (min)	19.6 (±2.1)	20.9
Y	Final Temperature (°C)	36.2 (±3.1)	36.8
	Time Constant (min)	27.1 (±3.0)	28.1
Z	Final Temperature (°C)	116.5 (±4.4)	118.6
	Time Constant (min)	6.0 (±0.9)	5.5

B. Application of characterisation and methodology for transient temperature response

The resulting thermal characterisation from the methodology described provides a relationship between sample thickness and thermal transfer for larger sample sizes where the effects of localised variations in material properties become negligible. This enables the estimation of the time taken for a section of CFRP to reach a particular temperature, for different thicknesses of CFRP material.

A specific application of the derived thermal characterisation is the case where an EPS which is integrated into a CFRP layup has a high operating temperature [2, 11, 12]. A typical layup of a CFRP inner wing support stringer cross section is illustrated in Fig. 8, with cabling routed along the spar centreline (cabling used in more-electric aircraft typically use 3 core AWG 4/0 with a diameter of 1cm for each cable). Including the inner and outer shielding and structural brackets, the approximate surface contact area between the cable sand spar is 0.7 m^2 for a 1m section of cable. During periods of maximum power, the outer shielding at the interface between the cable and the spar will reach in 150°C. This thermal energy will be conducted onto the surface of the spar. Ambient temperature is assumed to be 20°C.

If the spar to which the cable is attached is 52 plies thick (6.5 mm) and is made of using Hexply 8552 [0°] and heated to 150°C, it is possible to determine the effect of the heated cable on the spar using the derived ply-thermal relationship. Initially, Eq. 5 is used to determine the value of the coefficients (*a, b, c, d*) by using the 12 derived relationships for each coefficient and each axis direction as shown in Fig. 8. Once these are known, they can be used in Eq. 4 to create the thermal response equations for the axes with respect to time. This allows the final temperature response to be evaluated and the time constant, allowing the impact of heat transfer onto CFRP components to be understood.

The implementation of the ply-thermal relationship is summarised in Fig. 8 and would be repeated for different values of ply thickness. The thermal characterisation would predict, for a 52 ply spar, that the opposing surface temperature (z-axis) would reach a steady state of 124.5°C when the cable temperature in contact is 150°C, with a time constant of 480 s. Using (3) with a cross sectional area of 0.7 m^2, thermal conductivity of 0.78 W/m°C [63], a depth of 6.5 mm for a 52 ply layup and an ambient temperature of 20°C, the power dissipated on the opposite face per spar meter length would be 14.9kW. If the spar thickness was increased to 104 plies, the dissipated power would reduce to 7.5kW, highlighting the effect of part geometry on the localised heating. Other factors would influence the heat transfer and dissipation, for example fuel lines or other electrical control systems, however the derived relationship can inform the design of the aircraft in more electric settings. The increase in temperature in the Z axis would be of chief concern as the design of these spars is to allow communication and fuel channels to be routed along the length of the wing.

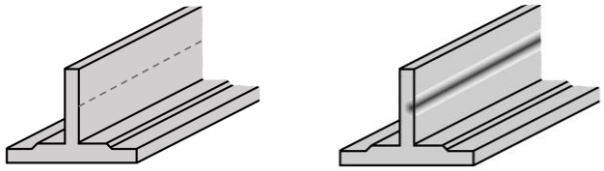

(a) **(b)**

***n* = 52**	**Direction**		
Coefficient Value (Derived Using Eq. 5)	**x-axis**	**y-axis**	**z-axis**
a	40.1	29.7	125
b	-0.152×10^{-5}	-0.253×10^{-5}	-0.0164×10^{-5}
c	-23.4	-12.2	-137
d	-0.0523	-0.0455	-0.241
Thermal Response (Derived Using Eq. 4)	$f(t) = 40.1\cdot\exp(-1.52\times10^{-6}\cdot t) - 23.4\cdot\exp(-0.0523\cdot t)$	$f(t) = 29.7\cdot\exp(-2.53\times10^{-6}\cdot t) - 12.2\cdot\exp(-0.0455\cdot t)$	$f(t) = 125\cdot\exp(-1.64\times10^{-7}\cdot t) - 137\cdot\exp(-0.241\cdot t)$
Final Temperature Response Along Axes (°C)	40.8	29.6	124.5

Fig. 8. *Above (a)* - Bay stringer wing cover support with integrated electrical protection cabling secured to surface of spar (vertical support), spar ply thickness is 52 plies [0°] CFRP. *Above (b)* – Electrical fault inducing heating in spar due to surface contact. *Lower*– Calculation of steady state induced temperature.

Without sufficient understanding of the potential thermal effects of integrated power systems in more-electric aircraft, the impact of high temperature cable operation and the even higher cable temperatures induced in response to fault conditions.

VII. Conclusions

This paper has demonstrated a method to characterise macro-scale CFRP layups of different component geometries, to derive coefficients that allow the transient thermal response of the material (for a pre-determined range of geometries) to be evaluated. The presented case study detailed the application of this characterisation process for the integration of on-board electrical power systems with CFRP structures. The methodology to derive thermal characterisation of UD [0º] CFRP presented relates thermal transfer to sample thickness based on UD [0º] CFRP, enabling an estimation of the expected thermal transfer within the given conditions, and upper and lower limits of the material dimensions. Therefore, the resulting thermal characterisation will inform the design and operation of aircraft EPS, supporting the development of appropriate electrical protection systems, the physical layout of the EPS and design of appropriate thermal management systems. The level of complexity of the resulting thermal characterisation is such that it can be integrated with appropriate systems level simulation studies of an aircraft EPS. Furthermore, the thermal characterisation also provides an opportunity to estimate the thermal response of Joule heating due to electrical conduction in the CFRP, informing the design limits for the integration of CFRP structures with the EPS, and subsequently enabling the design of integrated EPS-composite structures.

The methodology presented in this paper, also provides the basis for the future development of aerospace component-scale thermal characterisations for more complex layups, including woven CFRP. From the literature, thermal models of woven CFRP have been developed using similar, multi-scale numerical methods to those developed for UD CFRP e.g. [24], [64], Similar to UD CFRP, these models have not been developed into a form suitable for integration with systems level studies of aircraft EPS. It is known that additives such as carbon nanotubes or graphene offer an option to improve the thermal and electrical conductivity of CFRP [65], [66]. This would provide a database of thermal characterisations for different layups of CFRP to inform the selection of an appropriate CFRP lay-up and geometry for an integrated design process based on thermal requirements for the optimised design of the full system (EPS and CFRP structure). This database would also include an indication of the sensitivity of each thermal response to both layups by different manufacturers, and different layup parameters such as fibre orientation, weave and resin matrix.

Future analysis of scaled complex geometry components that are representative of full scale aero-structures would also provide understanding of the dominant thermal transfer characteristics of these parts. If thermal characterisation at fidelity compatible with systems modelling of aircraft EPS for these variants of CFRP can be developed, then this has potential to offer opportunity to fully optimise the integration of electrical power systems, and appropriate electrical protection system design, with CFRP structures on future aircraft systems.

Acknowledgement

The authors wish to acknowledge the support of Mike Jones from the Bristol Composites Institute, University of Bristol, Bristol, UK for manufacturing and supplying the samples of CFRP for the experiments described in this paper.

References

[1] M. Terorde, H. Wattar, and D. Schulz, “Phase balancing for aircraft electrical distribution systems,” *IEEE Trans. Aerosp. Electron. Syst.*, 2015.

[2] C. E. Jones *et al.*, “Electrical and thermal effects of fault currents in aircraft electrical power systems with composite aero-structures,” *IEEE Trans. Transp. Electrif.*, 2018.

[3] K. Takahashi and H. T. Hahn, “Investigation of temperature dependency of electrical resistance changes for structural management of graphite/polymer composite,” *J. Compos. Mater.*, 2011.

[4] SAE International, “Wiring Aerospace Vehicle, AS50881 F.” 2015.

[5] European Avaiation Safety Agency, “Certification Specifications and Acceptable Means of Compliance for Large Aeroplanes CS-25 (Large Aeroplanes).” 2017.

[6] J. R. Gaier, “Intercalated Graphite Fiber Composites as EMI Shields in Aerospace Structures,” *IEEE Trans. Electromagn. Compat.*, 1992.

[7] S. M. Braden and M. . Doherty, “Current return network,” 803148 B2, 2011.

[8] C. Lochot and D. Slomianowski, “A350 XWB Electrical Structure Network,” *Airbus Technical Magazine*, pp. 20–25, 2014.

[9] M. Gagné and D. Therriault, “Lightning strike protection of composites,” *Prog. Aerosp. Sci.*, 2014.

[10] J. Dalton and P. Broughton, “Rigid raft,” 0160460 A1, 2013.

[11] A. Piche, D. Andissac, I. Revel, and B. Lepetit, “Dynamic electrical behaviour of a composite material during a short circuit,” in *10th International Symposium on Electromagnetic Compatibility*, 2011, pp. 128–132.

[12] J. Rivenc, R. Perraud, T. Zink, D. Andissac, R. Mills, and J. Cinquin, “A multiphysic approach to predict the degradation of a composite material due to current injection,” in *17th European Conference on Composite Materials*, 2016.

[13] J. Rivenc, “Methodology for predicting degradation shape and depth of a CFRP during short - circuit current injection,” in *More Electric Aircraft Conference*, 2015.

[14] O. I. Zhupanska and R. L. Sierakowski, “Electro-thermo-mechanical coupling in carbon fiber polymer matrix composites,” *Acta Mech.*, 2011.

[15] G. Wasselynck, D. Trichet, and J. Fouladgar, “Determination of the electrical conductivity tensor of a CFRP composite using a 3-D percolation model,” *IEEE Trans. Magn.*, 2013.

[16] T. Schroter and D. Schulz, “The electrical aircraft networkbenefits and drawbacks of modifications,” *IEEE Trans. Aerosp. Electron. Syst.*, 2013.

[17] N. Yue, Y. Li, M. Bai, and S. Hou, “Flammable fluid fire protection airworthiness design and verification method of civil transport aircraft,” in *Procedia Engineering*, 2014.

[18] J. L. Rotgerink, H. Schippers, J. Verpoorte, and K. Nuyten, “EMC aspects of compact wiring for future aircraft,” in *2018 IEEE International Symposium on Electromagnetic Compatibility and 2018 IEEE Asia-Pacific Symposium on Electromagnetic Compatibility, EMC/APEMC 2018*, 2018.

[19] SAE International, “AIR6326 - Aircraft Electrical Power Systems Modelling and Simulation Definitions.” 2015.

[20] F. Gori and S. Corasaniti, “Effective thermal conductivity of composites,” *Int. J. Heat Mass Transf.*, 2014.

[21] M. Wang, Q. Kang, and N. Pan, “Thermal conductivity enhancement of carbon fiber composites,” *Appl. Therm. Eng.*, 2009.

[22] M. Wang, J. He, J. Yu, and N. Pan, “Lattice Boltzmann modeling of the effective thermal conductivity for fibrous materials,” *Int. J.*

Therm. Sci., 2007.
[23] K. Dong, B. Gu, and B. Sun, "Comparisons of thermal conductive behaviors of epoxy resin in unidirectional composite materials," *J. Therm. Anal. Calorim.*, 2016.
[24] K. Dong, K. Liu, Q. Zhang, B. Gu, and B. Sun, "Experimental and numerical analyses on the thermal conductive behaviors of carbon fiber/epoxy plain woven composites," *Int. J. Heat Mass Transf.*, 2016.
[25] E. P. Scott and J. V. Beck, "Estimation of Thermal Properties in Epoxy Matrix/Carbon Fiber Composite Materials," *J. Compos. Mater.*, 1992.
[26] Z. Fang *et al.*, "Geometrical Effect on Thermal Conductivity of Unidirectional Fiber-Reinforced Polymer Composite along Different In-plane Orientations," *Appl. Compos. Mater.*, 2018.
[27] P. Kosbe and P. A. Patil, "Effective thermal conductivity of polymer composites: a review of analytical methods," *Int. J. Ambient Energy*, 2018.
[28] H. J. Park, T. A. Kim, R. Kim, J. Kim, and M. Park, "A new method to estimate thermal conductivity of polymer composite using characteristics of fillers," *J. Appl. Polym. Sci.*, 2013.
[29] S. Hind and F. Robitaille, "Measurement, modeling, and variability of thermal conductivity for structural polymer composites," *Polym. Compos.*, 2010.
[30] K. Marlett, "Hexcel 8552 IM7 Unidirectional Pre-preg 190 gsm & 35% RC Qualification Material Property Data Report," 2011.
[31] F. H. Gojny *et al.*, "Evaluation and identification of electrical and thermal conduction mechanisms in carbon nanotube/epoxy composites," *Polymer (Guildf).*, 2006.
[32] C. Soutis, "Carbon Fiber Reinforced Plastics in Aircraft Construction," *Mater. Sci. Eng. A*, vol. 412, pp. 171–176, 2005.
[33] D. P. H. Hasselman and L. F. Johnson, "Effective Thermal Conductivity of Composites with Interfacial Thermal Barrier Resistance," *J. Compos. Mater.*, 1987.
[34] K. Potter, B. Khan, M. Wisnom, T. Bell, and J. Stevens, "Variability, fibre waviness and misalignment in the determination of the properties of composite materials and structures," *Compos. Part A Appl. Sci. Manuf.*, 2008.
[35] K. D. Potter, "Understanding The Origins of Defects And Variability in Composites Manufacture," *17 th Int. Conf. Compos. Mater.*, 2009.
[36] A. L. Stewart and A. Poursartip, "Characterization of fibre alignment in as-received aerospace grade unidirectional prepreg," *Compos. Part A Appl. Sci. Manuf.*, 2018.
[37] A. H. Muliana and J. S. Kim, "A two-scale homogenization framework for nonlinear effective thermal conductivity of laminated composites," *Acta Mech.*, 2010.
[38] J. R. Gaier, Y. YoderVandenberg, S. Berkebile, H. Stueben, and F. Balagadde, "The electrical and thermal conductivity of woven pristine and intercalated graphite fiber-polymer composites," *Carbon N. Y.*, 2003.
[39] "Aircraft Electrical Systems," *Acceptable methods, techniques, and practices – Aircraft inspection and repair*. 1998.
[40] K. Pietrak and T. S. Winiewski, "A review of models for effective thermal conductivity of composite materials," *J. J. Power Technol.*, 2015.
[41] G. S. Springer and S. W. Tsai, "Thermal Conductivities of Unidirectional Materials," *J. Compos. Mater.*, vol. 1, no. 2, pp. 166–173, 1967.
[42] S. D. McIvor *et al.*, "Thermal conductivity measurements of some glass fibre- and carbon fibre-reinforced plastics," *J. Mater. Sci.*, 1990.
[43] J. Llorca *et al.*, "Multiscale modeling of composite materials: A roadmap towards virtual testing," *Adv. Mater.*, 2011.
[44] J. J. Gou, C. L. Gong, L. X. Gu, S. Li, and W. Q. Tao, "Unit cells of composites with symmetric structures for the study of effective thermal properties," *Appl. Therm. Eng.*, 2017.
[45] R. Rolfes and U. Hammerschmidt, "Transverse thermal conductivity of CFRP laminates: A numerical and experimental validation of approximation formulae," *Compos. Sci. Technol.*, 1995.
[46] S. Bensaid, D. Triebet, and J. Fouladgar, "3-D simulation of induction heating of anisotropic composite materials," in *IEEE Transactions on Magnetics*, 2005.
[47] B. Sarlioglu and C. T. Morris, "More Electric Aircraft: Review, Challenges, and Opportunities for Commercial Transport Aircraft," *IEEE Trans. Transp. Electrif.*, 2015.
[48] P. Wheeler, "Technology for the more and all electric aircraft of the future," in *2016 IEEE International Conference on Automatica, ICA-ACCA 2016*, 2016.
[49] B. Karanayil, M. Ciobotaru, and V. G. Agelidis, "Power flow management of isolated multiport converter for more electric aircraft," *IEEE Trans. Power Electron.*, 2017.
[50] M. W. Pilling, B. Yates, M. A. Black, and P. Tattersall, "The thermal conductivity of carbon fibre-reinforced composites," *J. Mater. Sci.*, 1979.
[51] "Standard Test Method for Thermal Conductivity and Thermal Diffusivity by Modulated Temperature Differential Scanning Calorimetry," 2017.
[52] W. J. Parker, R. J. Jenkins, C. P. Butler, and G. L. Abbott, "Flash method of determining thermal diffusivity, heat capacity, and thermal conductivity," *J. Appl. Phys.*, 1961.
[53] M. Villière, D. Lecointe, V. Sobotka, N. Boyard, and D. Delaunay, "Experimental determination and modeling of thermal conductivity tensor of carbon/epoxy composite," *Compos. Part A Appl. Sci. Manuf.*, 2013.
[54] "Standard Test Method for Thermal Transmission Properties of Thermally Conductive Electrical Insulation Materials," 2017.
[55] "Standard Test Method for Steady-State Thermal Transmission Properties by Means of the Heat Flow Meter Apparatus," 2017.
[56] "Standard Test Method for Steady-State Heat Flux Measurements and Thermal Transmission Properties by Means of the Guarded-Hot-Plate Apparatus," 2013.
[57] Antonio Visioli, "The Tuning Issue," in *Practical PID Control*, London: Springer-Verlag, p. 17.
[58] B. Liptak, Ed., "Resistance Temperature Detectors," in *Process Measurement and Analysis*, 4th ed., Boca Raton, 2003, pp. 587, 647.
[59] F. Ohnhäuser, "Introduction," in *Analog-Digital Converters for Industrial Applications Including and Introduction to Digital-Analog Converters*, Berlin: Springer-Verlag, 2015, p. 24.
[60] K. A. Seeler, *System Dynamics - An Introduction for Mechanical Engineers*. 2014.
[61] N. Ersoy and M. Tugutlu, "Cure kinetics modeling and cure shrinkage behavior of a thermosetting composite," *Polym. Eng. Sci.*, 2010.
[62] T. MathWorks, "MATLAB (R2017b)," *The MathWorks Inc.* 2017.
[63] S. Eibl, "Influence of carbon fibre orientation on reaction-to-fire properties of polymer matrix composites," *Fire Mater.*, 2012.
[64] A. Dasgupta and R. K. Agarwal, "Orthotropic Thermal Conductivity of Plain-Weave Fabric Composites Using a Homogenization Technique," *J. Compos. Mater.*, 1992.
[65] S. Han and D. D. L. Chung, "Increasing the through-thickness thermal conductivity of carbon fiber polymer-matrix composite by curing pressure increase and filler incorporation," *Compos. Sci. Technol.*, 2011.
[66] A. Warrier *et al.*, "The effect of adding carbon nanotubes to glass/epoxy composites in the fibre sizing and/or the matrix," *Compos. Part A Appl. Sci. Manuf.*, 2010.